MODELLING THE PROCESS OF FUSED DEPOSITION MODELLING AND THE EFFECT OF TEMPERATURE ON THE MECHANICAL, ROUGHNESS, AND POROSITY PROPERTIES OF RESULTING COMPOSITE PRODUCTS

K. Abouzaid,[1] D. Bassir,[2,3*] S. Guessasma,[4] and H. Yue[5]

Advances in the additive manufacturing (AM) processes have opened up the possibilities of widely using them in various structural sectors. Since 1980s this technology has been in permanent mutations. The ramification of the AM technology makes it difficult to obtain a clear impression of its potentialities. Predicting and controlling the mechanical characteristics of printed products is crucial for their final practical use. This study mainly aims to characterize the impact of printing parameters on the characteristics of printed articles and to evaluate their significance.

1. Introduction

The Additive Manufacturing (AM) is a sophisticated technology used for three-dimensional processing by joining materials, usually layer by layer. This process offers the benefit of creating any complex object starting from a 3D representation of its external surface. It goes with a short realization time, cost efficiency, and minimum need for tooling. A wide variety of materials can be used in this process, such as ceramics, polymers, metals, alloys, and composites [1,

[1]INRAE, Avignon University, UMR EMMAH, F-84000, Avignon, France.
[2]CNRS/UMR 5060, / Univ. Bourgogne Franche Comté (UBFC)-UTBM, France
[3]Borelli Center, UMR 9010, ENS Cachan, Université Paris-Saclay, 94235 Cachan, France
[4]INRA, UR1268 Biopolymères Interactions Assemblages, F-44300 Nantes, France
[5]FRDISI, National and High School of Electricity and Mechanics, Hassan II University, Morocco
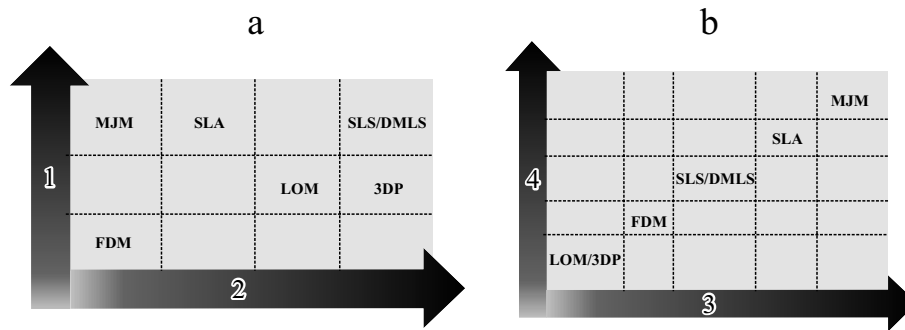*Corresponding author; e-mail: david.bassir@gmail.com

Fig. 1. AM classification based on the Main machine characteristics (a) and esthetic features (b): 1 — build cost, 2 — build speed, 3 — dimensional accuracy, and 4 — surface quality.

2], which allow them to invade different industrial sectors including, aerospace [3], building [4-6], biomedical [7-10], education [11], and also to use it for personal needs, such as art and hobbies.

Actually, the AM is the most usable manufacturing process in medical industry to combat the recent pandemic (Covid-19 virus) [12-14]. New AM applications have appeared to withstand this virus, such as manufacturing medical face masks.

In a few recent years, the range of AM feedstock has been enlarged significantly by adding new materials to it, such as nanoparticles and smart and biobased materials to expand and to strengthen its application domains by helping in the protection of environment [2, 15-19].

The AM includes a large number of processes. All they differ in the principle of operation, the layer deposition manner, and the materials used to produce parts. There are three different categories of AM processes — liquid-, solid-, and powder-based ones. Depending on these categories, the material transformation process ranges from polymerization, binding, to melting [20]. In Fig. 1, the AM processes are compared in terms of material and product characteristics [2, 21-23]. The cost and speed are among the primary considerations when choosing an adequate printing machine. The Fused Deposition Modelling (FDM) is the least expensive process, with a low expenditure of energy. For this reason, it is the main technique used nowadays, especially to improve the quality of FDM-printed products, including their mechanical and thermal characteristics.

This article reflects the challenges regarding the parameter identification of printed products and the sensitivity analysis of the parameters affecting their quality the most. It also analyzes their main characteristics, including surface quality, porosity, and mechanical features.

2. Fused Deposition Modelling (FDM)

The FDM is an additive manufacturing process where thin filaments of a plastic material are used to build objects by adding their layers. It was patented by Scott Crump in 1988 [24] and commercialized by Stratasys in the USA. The FDM printing process begins with adjustment of the melting temperature. Then, the machine is fueled with a filament feedstock, which is pushed to the heated liquefier via a stepper motor to a pinch roller mechanism to be melted there. The different steps of the feeding process present multiple mechanical and thermal actions (tension, compression, and heating). The melted material obtained is then extruded selectively through a small print nozzle that traces the cross-sectional geometry of parts by roads or by beads given by the STL model (Fig. 2) [25-27].

The nonlinearity of the melt properties generated during printing mainly depends on its temperature and shear rate. The feedstock feed rate is controlled in the liquefier in order to maintain the volumetric flow rate constant. The melt flow in the liquefier is described by the generalized Newtonian power law
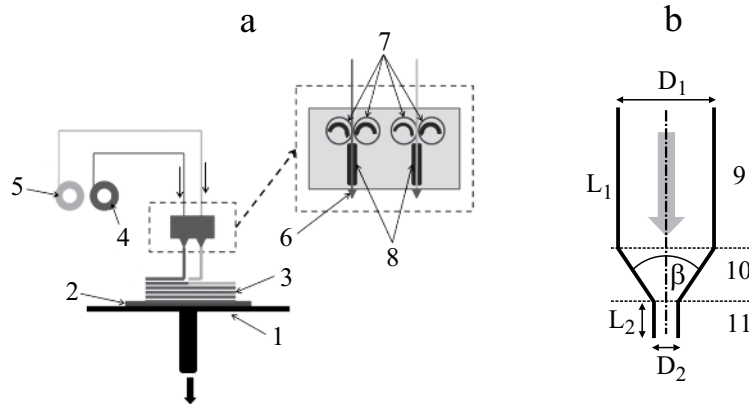
Fig. 2. Fused deposition modelling (FDM) (a) and nozzle geometry (b): 1 — build platform, 2 — foam base, 3 — part, 4 — build material filament spool, 5 — support material filament spool, 6 — print nozzle, 7 — feed pinch rollers, 8 — heated liquefier, 9 — section 1, 10 — section 2, and 11 — section 3.
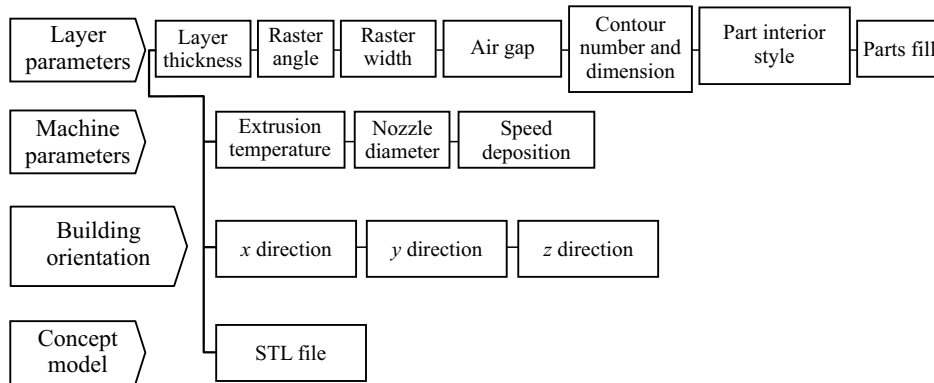

Fig. 3. Principal FDM process parameters.

$$\tau = \left(\frac{\dot{\gamma}}{\Phi} \right)^{1/m} ,$$

where τ is the shear stress, $\dot{\gamma}$ is the shear rate, and m and Φ are material constants.

The liquefier geometry is divided into different sections, as shown in Fig. 2 [28], and the temperature variation during and after the extrusion process is described by the equation

$$\rho c_p \frac{\partial T}{\partial t} = \lambda \left(\frac{\partial^2 T}{\partial x^2} + \frac{\partial^2 T}{\partial y^2} + \frac{\partial^2 T}{\partial z^2} \right) ,$$

where ρ, c_p, and λ are the density, the specific heat capacity (at a constant pressure), and the coefficient of thermal conductivity, respectively.

Furthermore, the latent heat in the transition phase of polymers during the extrusion process also cannot be ignored. The enthalpy in this case is

$$H = \int \rho C(T) dT ,$$

where ρ is the density, C is the specific heat, and T is temperature
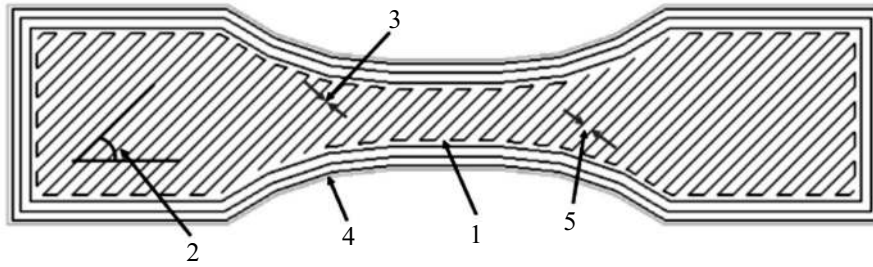
807

Fig. 4. FDM tool path parameters: 1 — raster, 2 — raster angle, 3 — raster width, 4 — perimeter, and 5 — air gap.

3. Parameter Analysis and Discussion

Many researchers have investigated the properties of parts made by the FDM and the process parameters characterizing the deposited layer geometries, which are presented in Figs. 3 and 4.

3.1. Surface roughness and porosity

Among the critical properties of FDM products treated are their surface quality and dimensional accuracy [29]. According to the recent reports and results, the surface roughness is affected most by the layer thickness, followed by the raster width and building orientation of a part [30]. The latter parameter greatly affects the dimensional accuracy, followed by the layer thickness [31]. A small layer thickness, as well as a small raster width of filaments, improves the surface quality.

A void between deposited filaments, called "air gap", which is a crucial parameter of the final part of FDM, has a greater impact on the dimensional accuracy than the surface roughness. There are three types of air gaps. A positive air gap means the presence of a void between roads, a zero gap means that there are no voids between them (they touch each other), and a negative one means that roads overlap. The porosity of a part is indispensable in the case of FDM-mode products, due to the manufacturing method based on road deposition next to each other. The use of negative air gap factors may decrease the porosity, which reduces dimensional errors, but impairs the surface quality of final parts [32]. Therefore, to achieve a minimum dimensional error and ensure a good surface quality, it is recommended to use the following combination: a small layer thickness, an average raster width, a zero air gap, and the 0°/90° orientation of rods [33]. Besides, some esthetic defects can be removed by postprocessing techniques, including mechanical ones, such as the milling, the CNC, the abrasive or vibratory bowl machining, or chemical techniques by applying vapor or a slight amount of acetone to dissolve the rough or porous parts in order to achieve the best final quality [34].

The effect of raster angle on the esthetic properties of final parts have also been investigated. It is found that the effect of this parameter depends on the material printed. Generally, the +45°/–45° angles have found to give the best surface quality and dimensional accuracy [35]. The aesthetic properties of final FDM products depend mainly on the layer thickness and printing orientation.
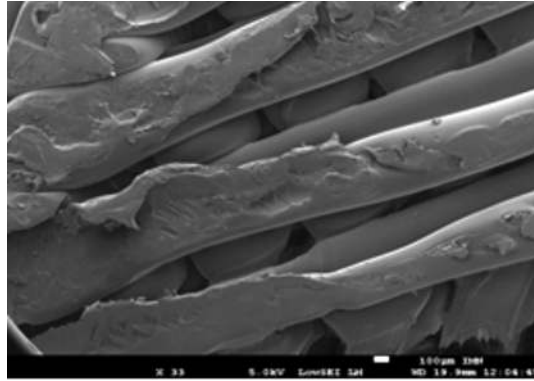
Fig. 5. Low adhesion along the junction between layers in a FDM-printed part [54].

3.2. Mechanical properties

When printing functional parts, their crucial features are Young's modulus, the ultimate tensile strength, yield strength, and ductility. These parameters influence the mechanical properties of FDM-made parts to different degrees.

It is worth mentioning that the main FDM parameter to obtain a functional part is the part fill that specifies the percentage of material [36-38]. This parameter should be fixed at high values, which are linked to negative values of the air gap parameter.

There exists an extensive range of FDM feedstock materials, of which acrylonitrile butadiene styrene (ABS) and polylactic acid (PLA) have been widely studied owing to their good mechanical properties. A literature survey shows that up to 2/3 of the studies reported concern exactly these two materials. It reveals that the building orientation and raster angle are the factors that influence the tensile properties of products, including Young's modulus, the ultimate tensile strength, and ductility most significantly, followed by the layer thickness and other FDM parameters. Building ABS and PLA parts in the plane direction is the optimal direction to ensure the highest Young's modulus [39-41], but the impact of raster angle is substantially different. The highest ultimate strength is obtained by printing at 45° and 0°/90° angles for PLA [40] and ABS [42, 43] samples, respectively. The layer thickness is also an important input parameter affecting their tensile properties. It has been shown that small layer thicknesses (less than 1 mm) are the most adequate to realize FDM-made parts with good mechanical characteristics [36, 39, 40, 44]. The interlayer and interraster bondings are among the weakest ones in the FDM process. Therefore, the raster width should be great to cover the full adhesion surface in order to ensure a high degree of cohesion in the part [40, 45].

The FDM feedstock is not restricted to ABS and PLA materials. There are several polymers that are also classified as stiff and strong FDM materials, e.g., polycarbonate (PC), polypropylene (PP), PEEK, UTEM, and polyamide (PA).

For PC, PEEK, and PLA, the same raster angles and building orientation are recommended [38, 42]. PP, PA and UTEM 9085 are similar to ABS, for which the zero raster angle is the best to reach a high Young's modulus and the ultimate tensile strength [46-49].

As for the fracture toughness, it is highest at the zero raster angle, which may increase the fracture toughness K_c to about 2 and 5 MPa·m$^{1/2}$ for ABS [50-52] and PLA [44] respectively. The fracture toughness can also be improved by increasing the roughness degree of material mixture, because the grains present in the material tend to resist crack growth [53].
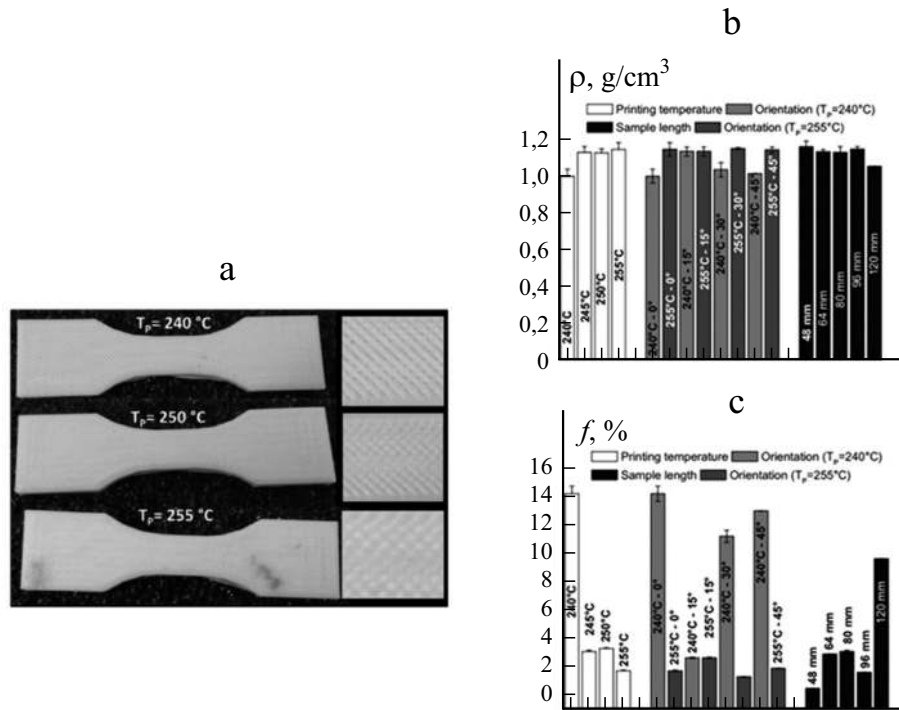
Fig. 6. Filament cohesiveness at various printing temperatures (a) and the apparent density ρ (b) and porosity f (c) as functions of printing temperature [64].

3.3. Impact of printing temperature

Much attention has been focused on finding the optimal tool path parameters and on clarifying their impact on the printing pattern and the 3D-printing object. But the relation between these printing parameters and the printing temperature is often neglected. One of the major concerns related to the fused deposition modelling process is to maintain an adequate printing temperature to ensure a smooth printing operation.

An inadequate extrusion temperature range can damage the product. Low temperatures can lead to a low layer adhesion (Fig. 5), peeling off of layers, and even nozzle clogging. At a high printing temperature, large thermal gradients can arise, and attempts to of maintain a constant layer height can alter the desirable geometry of parts [31, 54].

In all conditions, high or moderate temperatures are recommended. An increased temperature raises the average temperature between layers, and more time above T_g is spent, which improves the interlayer welding. Moreover, the raster angle and width become more adjusted and ensure a high adhesion in layers [55-57]. The layers are flattened, and the surface roughness of the whole part decreases.

The anisotropy of printed parts is better controllable at high printing temperatures. The voids in the mesostructure with a cross-linked filament arrangement is the principal factor increasing the porosity f [58-60]

A low temperature hinders the adequate flow deposition through the nozzle and may generate discontinuous rasters and decrease the cohesiveness between the deposited filaments. A high printing temperature decreases the porosity of printed parts by minimizing the thermal transfers of deposited rasters and maximizing the cooling time during the printing operation (Fig. 6) [61]. Guessasma [62] confirmed the existence of this phenomenon and proposed an approximate formula for the porosity f and the printing temperature T_p based on microtomography measurements, namely,
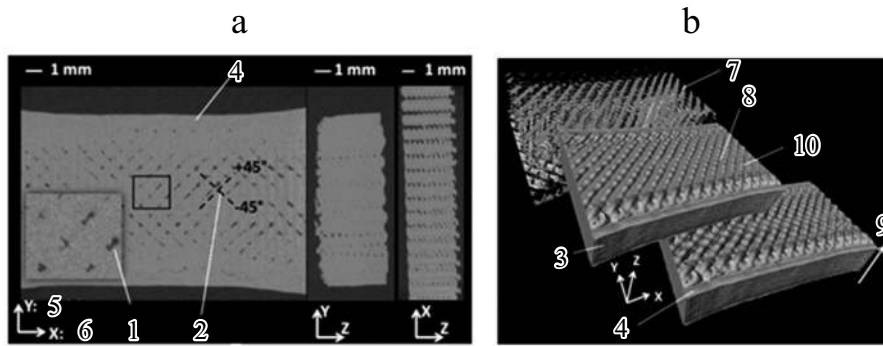
$$f(\%) = 19.2 - 0.06 T_p(°C)$$

Fig. 7. The porosity f of a 3D-printed PLA revealed by the X-ray microtomography: cross-sectional views (a) and porosity network arrangement (b) [62]: 1 — void, 2 — raster, 3 — layer, 4 — frame, 5 — width, 6 — length, 7 — porosity network, 8 — surface porosity, 9 — building direction, and 10 — PA filament.
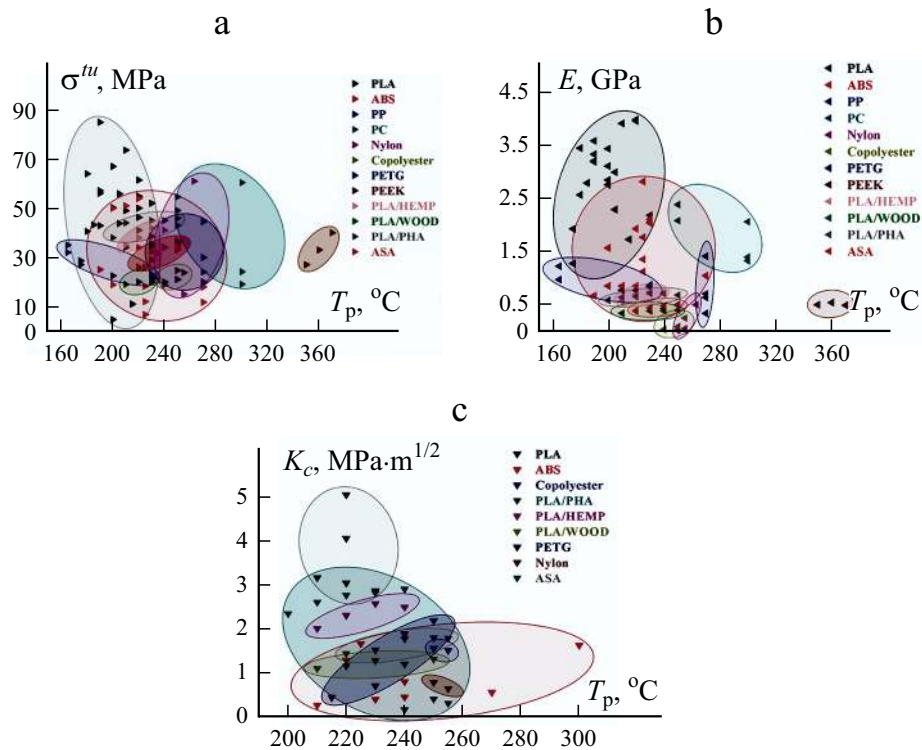

Fig. 8. Uniaxial tensile strength (UTS) (a), Young's modulus E (b), and fracture toughness K_c (c) as a functions of printing temperature T_p.

This linear model shows that pores are not distributed arbitrarily in the printed part — they are concentrated at the intersection of printed rasters (Fig. 7).

The printing temperature strongly correlates with mechanical properties, with anisotropy of the printed pattern being the main reason for its mechanical weakness. As already mentioned, a high printing temperature improves the interfilament welding and leads to a high adhesion between layers [61, 63, 64], which increases the elastic modulus and tensile strength. A summary of the results of literature studies is presented in Fig. 8, where it is shown that the mechanical properties of different

FDM-made polymer composites depend on printing temperature [31, 38, 39, 42-44, 46, 48, 50-52, 54, 64-73]. Further investigations are needed to determine the optimal values of FDM process parameters by employing various design optimization methods and techniques [74-78].

4. Conclusion

The first part of this article was dedicated to an overview of the additive manufacturing and fused deposition processes. Various printing parameters and their influence on the quality of printed patterns were considered and recent results of temperature influence on their roughness and porosity during the FDM process were judged.

The crucial factors to be taken into account before building a part were examined, and it was found that the most significant ones were those related to tool path parameters, such as the layer thickness and part building orientation.

The influence of the principal printing parameter was described by a theoretical model characterizing the thermal behavior of parts during the printing process. Finally, the impact of printing temperature on the porosity and the mechanical behavior of printing polymers was summarized.

Nonetheless, there still are a few impediments which hinder one to obtain a product with excellent mechanical properties. The control of porosity of printed parts, which worsens their mechanical properties is still a problem. Voids in deposited trajectories and between layers reduce cohesion and, as result, small cracks may appear and propagate in parts. Therefore, fatigue studies are required to obtain a further insight into this phenomenon.

REFERENCES

1. S. Guessasma, W. Zhang, J. Zhu, et al., "Challenges of additive manufacturing technologies from an optimisation perspective," International Journal for Simulation and Multidisciplinary Design Optimization, **6**, A9 (2015).
2. T. D. Ngo, A. Kashani, G. Imbalzano, K. T. Q. Nguyen, and D. Hui, "Additive manufacturing (3D printing): A review of materials, methods, applications and challenges," Composites Part B: Engineering, **143**, 172-196 (2018).
3. L. J. Kumar and C. K. Nair, "Current trends of additive manufacturing in the aerospace industry,". In : Advances in 3D printing & additive manufacturing technologies, Springer, Singapore (2017). pp. 39-54.
4. A. Nadal, J. Pavón, and O. Liébana, "3D printing for construction: a procedural and material-based approach," Informes de la Construcción, **69**, 546, e193, (2017).
5. Y. W. D. Tay, B. Panda, S. C. Paul, et al., "3D printing trends in building and construction industry: a review," Virtual and Physical Prototyping, **12**, No. 3, 261-276 (2017).
6. J. Xu, L. Ding, and P. E. Love, "Digital reproduction of historical building ornamental components: From 3D scanning to 3D printing," Automation in Construction, **76**, 85-96 (2017).
7. A. S. Mangat, S. Singh, M. Gupta, et al., "Experimental investigations on natural fiber embedded additive manufacturing-based biodegradable structures for biomedical applications," Rapid Prototyping Journal, **24**, 1221-1234 (2018).
8. J. Avila, S. Bose, and A. Bandyopadhyay, "Additive manufacturing of titanium and titanium alloys for biomedical applications," Titanium in Medical and Dental Applications, 325-343 (2018).
9. F. Liravi and E. Toyserkani, "Additive manufacturing of silicone structures: A review and prospective," Additive Manufacturing, **24**, 232-242 (2018).
10. M. Trivedi, J. Jee, S. Silva, et al., "Additive manufacturing of pharmaceuticals for precision medicine applications: A review of the promises and perils in implementation," Additive Manufacturing, **23**, 319-328 (2018).

11. S. Ford and T. Minshall, "Invited review article: Where and how 3D printing is used in teaching and education," Additive Manufacturing, **25**, 131-150 (2019).

12. R. Srinivasan, A. Mian, J. Gockel, et al., "Additive Manufacturing and How 3D Printing is Fighting COVID-19," Additive Manufacturing, **5**, 1-2020 (2020).

13. J. M. Zuniga and A. Cortes, "The role of additive manufacturing and antimicrobial polymers in the COVID-19 pandemic," Expert Review of Medical Devices, **17**, No. 6, 477-481(2020).

14. J. M. Pearce, "A review of open source ventilators for COVID-19 and future pandemics," F1000Research, **9**, 218 (2020).

15. J. Y. Lee, J. An, and C. K. Chua, "Fundamentals and applications of 3D printing for novel materials," Applied Materials Today, **7**, 120-133 (2017).

16. B. Bhushan and M. Caspers, "An overview of additive manufacturing (3D printing) for microfabrication," Microsystem Technologies, **23**, 1117-1124 (2017).

17. X. Wang, M. Jiang, Z. Zhou, J. Gou, and D. Hui, "3D printing of polymer matrix composites: A review and prospective," Composites Part B: Engineering, **110**, 442-458 (2017).

18. J. S. Cuellar, G. Smit, D. Plettenburg, et al., "Additive manufacturing of non-assembly mechanisms," Additive Manufacturing, **21**, 150-158 (2018).

19. D. Rejeski, F. Zhao, and Y. Huang, "Research needs and recommendations on environmental implications of additive manufacturing," Additive Manufacturing, **19**, 21-28 (2018).

20. C. Teng, D. Pal, H. Gong, K. Zeng, et al., "A review of defect modeling in laser material processing," Additive Manufacturing), **14**, 137-147 (2017).

21. L. J. Kumar, P. M. Pandey, and D. I. Wimpenny, "Comparison of bonding strength of Ti–6Al–4V alloy deposit and substrate processed by laser metal deposition," 3D Printing and Additive Manufacturing Technologies, Springer, 29-38, (2019)

22. W. T. Carter, M. G. Jones, L. Yuan et ,al., "Control of solidification in laser powder bed fusion additive manufacturing using a diode laser fiber array," U.S. Patent No. 10532556, Jan. 14, 2020.

23. F. Khodabakhshi, M. H. Farshidianfar, A. P. Gerlich, et al., "Effects of laser additive manufacturing on microstructure and crystallographic texture of austenitic and martensitic stainless steels," Additive Manufacturing, **31**, 100915 (2020).

24. S. S. Crump, "Apparatus and method for creating three-dimensional objects," U.S. Patent No. 5121329, June 9, 1992.

25. G. D. Goh, Y. L. Yap, H. Tan, S. L. Sing, G. L. Goh, and W. Y. Yeong, "Process–structure–properties in polymer additive manufacturing via material extrusion: A review," Critical Reviews in Solid State and Materials Sciences, **45**, 113-133 (2020).

26. H. Wu, W. Fahy, S. Kim, H. Kim, et al., "Recent developments in polymers/polymer nanocomposites for additive manufacturing," Progress in Materials Science, **111**, 100638 (2020).

27. S. Daminabo, S. Goel, S. Grammatikos, H. Nezhad, and V. K. Thakur, "Fused deposition modeling-based additive manufacturing (3D printing): techniques for polymer material systems," Materials Today Chemistry, **16**, 100248 (2020).

28. Y. Zhang and V. Shapiro, "Linear-time thermal simulation of as-manufactured fused deposition modeling components," Journal of Manufacturing Science and Engineering, **140**, 071002 (2018).

29. A. Qattawi and M. A. Ablat, "Design consideration for additive manufacturing: fused deposition modelling," Open Journal of Applied Sciences, **7**, 291 (2017).

30. E. Vahabli and S. Rahmati, "Improvement of FDM parts' surface quality using optimized neural networks–medical case studies," Rapid Prototyping Journal, **23**, 825-842 (2017).

31. S. Mahmood, A. Qureshi, and D. Talamona, "Taguchi based process optimization for dimension and tolerance control for fused deposition modelling," Additive Manufacturing, **21**, 183-190 (2018).

32. H. Nouri, S. Guessasma, and S. Belhabib, "Structural imperfections in additive manufacturing perceived from the X-ray micro-tomography perspective," Journal of Materials Processing Technology, **234**, 113-124 (2016).

33. P. K. Garg, R. Singh, and I. Ahuja, "Multi-objective optimization of dimensional accuracy, surface roughness and hardness of hybrid investment cast components," Rapid Prototyping Journal, **23**, 845-857 (2017).

34. J. S. Chohan and R. Singh, "Pre and post processing techniques to improve surface characteristics of FDM parts: a state of art review and future applications," Rapid Prototyping Journal, **23**, 495-513 (2017).

35. A. Armillotta and M. Cavallaro, "Edge quality in fused deposition modeling: I. Definition and analysis," Rapid Prototyping Journal, **23**, 1079-1087 (2017).

36. X. Zhou, S. J. Hsieh, and C. C. Ting, "Modelling and estimation of tensile behaviour of polylactic acid parts manufactured by fused deposition modelling using finite element analysis and knowledge-based library," Virtual and Physical Prototyping, **13**, No. 3, 177-190 (2018).

37. Y. Y. Aw, C. K. Yeoh, M. A. Idris, P. L. The, et al., "Effect of printing parameters on tensile, dynamic mechanical, and thermoelectric properties of FDM 3D printed CABS/ZnO composites," Materials, **11**, No. 4, 466 (2018).

38. X. Deng, Z. Zeng, B. Peng, et al., "Mechanical properties optimization of poly-ether-ether-ketone via fused deposition modeling," Materials, **11**, No. 2, 216 (2018).

39. J. Chacón, M. Caminero, E. García-Plaza, and P. Núñez, "Additive manufacturing of PLA structures using fused deposition modelling: Effect of process parameters on mechanical properties and their optimal selection," Materials & Design, **124**, 143-157 (2017).

40. X. Liu, M. Zhang, S. Li, L. Si, et al., "Mechanical property parametric appraisal of fused deposition modeling parts based on the gray Taguchi method," The International Journal of Advanced Manufacturing Technology, **89**, 2387-2397 (2017).

41. D. A. Türk, F. Brenni, M. Zogg, and M. Meboldt, "Mechanical characterization of 3D printed polymers for fiber reinforced polymers processing," Materials & Design, **118**, 256-265 (2017).

42. J. T. Cantrell, S. Rohde, D. Damiani, R. Gurnani, et al., "Experimental characterization of the mechanical properties of 3D-printed ABS and polycarbonate parts," Rapid Prototyping Journal, **23**, 811-824 (2017).

43. S. Mahmood, A. Qureshi, K. L. Goh, and D. Talamona, "Tensile strength of partially filled FFF printed parts: experimental results," Rapid Prototyping Journal, **23**, 122-128 (2017).

44. Y. Song, Y. Li, W. Song, K. Yee, et al., "Measurements of the mechanical response of unidirectional 3D-printed PLA," Materials & Design, **123**, 154-164 (2017).

45. M. S. Uddin, M. F. R. Sidek, M. A. Faizal, et al., "Evaluating mechanical properties and failure mechanisms of fused deposition modeling acrylonitrile butadiene styrene parts," Journal of Manufacturing Science and Engineering, **139**, No. 8, 081018, (2017).

46. M. Milosevic, D. Stoof, and K. Pickering, "Characterizing the Mechanical Properties of Fused Deposition Modelling Natural Fiber Recycled Polypropylene Composites," Journal of Composites Science, **1**, 1, 7 (2017).

47. L. Wang and D. J. Gardner, "Effect of fused layer modeling (FLM) processing parameters on impact strength of cellular polypropylene," Polymer, **113**, 74-80 (2017).

48. D. Stoof and K. Pickering, "Sustainable composite fused deposition modelling filament using recycled pre-consumer polypropylene," Composites Part B: Engineering, **135**, 110-118 (2018).

49. R. J. Zaldivar, D. B. Witkin, T. McLouth, et al., "Influence of processing and orientation print effects on the mechanical and thermal behavior of 3D-Printed ULTEM® 9085 Material," Additive Manufacturing, **13**, 71-80 (2017).

50. T. D. McLouth, J. V. Severino, P. M. Adams, D. N. Patel, and R. J. Zaldivar, "The impact of print orientation and raster pattern on fracture toughness in additively manufactured ABS," Additive Manufacturing, **18**, 103-109 (2017).

51. N. Aliheidari, R. Tripuraneni, A. Ameli, and S. Nadimpalli, "Fracture resistance measurement of fused deposition modeling 3D printed polymers," Polymer Testing, **60**, 94-101 (2017).

52. K. R. Hart and E. D. Wetzel, "Fracture behavior of additively manufactured acrylonitrile butadiene styrene (ABS) materials," Engineering Fracture Mechanics, **177**, 1-13 (2017).

53. V. Damodaran, A. G. Castellanos, M. Milostan, and P. Prabhakar, "Improving the Mode-II interlaminar fracture toughness of polymeric matrix composites through additive manufacturing," Materials & Design, **157**, 60-73 (2018).

54. K. Abouzaid, S. Guessasma, S. Belhabib, D. Bassir, and A. Chouaf, "Thermal mechanical characterization of copolyester for additive manufacturing using FDM," International Journal for Simulation and Multidisciplinary Design Optimization, **10**, A9 (2019).

55. D. J. Braconnier, R. E. Jensen, and A. M. Peterson, "Processing parameter correlations in material extrusion additive manufacturing," Additive Manufacturing, **31**, 100924 (2020).

56. T. J. Coogan and D. O. Kazmer, "Bond and part strength in fused deposition modeling," Rapid Prototyping Journal, **23**, No. 2, 414-422 (2017).

57. C. S. Davis, K. E. Hillgartner, S. H. Han, and J. E. Seppala, "Mechanical strength of welding zones produced by polymer extrusion additive manufacturing," Additive manufacturing, **16**, 162-166 (2017).

58. S. Guessasma, S. Belhabib, and H. Nouri, "Understanding the microstructural role of bio-sourced 3D printed structures on the tensile performance," Polymer Testing, **77**, 105924 (2019).

59. S. Guessasma, S. Belhabib, and H. Nouri, "Microstructure, Thermal and mechanical behavior of 3D printed acrylonitrile styrene acrylate," Macromolecular Materials and Engineering, **304**, No.7, 1800793 (2019).

60. S. G. Lekhnitskii, Elasticity Theory of Anisotropic Bodies [in Russian], Nauka, Moscow (1977).

61. S. Guessasma, S. Belhabib, and H. Nouri, "Printability and Tensile Performance of 3D Printed Polyethylene Terephthalate Glycol Using Fused Deposition Modelling," Polymers, **11**, No. 7, 1220 (2019).

62. S. Guessasma, S. Belhabib, and A. Altın, "On the Tensile Behaviour of Bio-sourced 3D-Printed Structures from a Microstructural Perspective," Polymers, **12**, No. 5, 1060 (2020).

63. A. A. D'Amico, A. Debaie, and A. M. Peterson, "Effect of layer thickness on irreversible thermal expansion and inter-layer strength in fused deposition modeling," Rapid Prototyping Journal, **23**, No. 5, 943-953 (2017).

64. K. Abouzaid, S. Guessasma, S. Belhabib, D. Bassir, and A. Chouaf, "Printability of co-polyester using fused deposition modelling and related mechanical performance," European Polymer Journal, **108**, 262-273 (2018).

65. A. N. Dickson, J. N. Barry, K. A. McDonnell, and D. P. Dowling, "Fabrication of continuous carbon, glass and kevlar fibre reinforced polymer composites using additive manufacturing," Additive Manufacturing, **16**, 146-152 (2017).

66. R. T. L. Ferreira, I. C. Amatte, T. A. Dutra, and D. Bürger, "Experimental characterization and micrography of 3D printed PLA and PLA reinforced with short carbon fibers," Composites Part B: Engineering, **124**, 88-100 (2017).

67. E. Gkartzou, E. P. Koumoulos, and C. A. Charitidis, "Production and 3D printing processing of bio-based thermoplastic filament," Manufacturing Review, **4**, No. 1 (2017).

68. Y. Jin, Y. Wan, B. Zhang, and Z. Liu, "Modeling of the chemical finishing process for polylactic acid parts in fused deposition modeling and investigation of its tensile properties," Journal of Materials Processing Technology, **240**, 233-239 (2017).

69. C. Koch, L. Van Hulle, and N. Rudolph, "Investigation of mechanical anisotropy of the fused filament fabrication process via customized tool path generation," Additive Manufacturing, **16**, 138-145 (2017).

70. N. G. Tanikella, B. Wittbrodt, and J. M. Pearce, "Tensile strength of commercial polymer materials for fused filament fabrication 3D printing," Additive Manufacturing, **15**, 40-47 (2017).

71. Z. Hou, X. Tian, J. Zhang, and D. Li, "3D printed continuous fibre reinforced composite corrugated structure," Composite Structures, **184**, 1005-1010 (2018).

72. H. Li, T. Wang, J. Sun, et al., "The effect of process parameters in fused deposition modelling on bonding degree and mechanical properties," Rapid Prototyping Journal, **24**, 80-92 (2018).

73. L. R. Lopes, A. F. Silva, and O. S. Carneiro, "Multi-material 3D printing: The relevance of materials affinity on the boundary interface performance," Additive Manufacturing, **23**, 45-52 (2018).

74. S. Bochkareva, N. Y. Grishaeva, B. A. Lyukshin, et al., "A unified approach to determining the effective physicomechanical characteristics of filled polymer composites based on variational principles," Mech. Compos. Mater., **54**, No. 6, 775-788 (2019).

75. E. Barkanov, A. Kovalov, P. Wierach, et al., "Optimized comparative analysis of an active twist for helicopter rotor blades with C-and D-spar designs," Mech. Compos. Mater., **54**, No. 5, 553-566 (2018).

76. T. Galichyan, A. Z. Khurshudyan, and D. FilippoV, "Parameter optimization of laminated multiferroic composites," Mech. Compos. Mater., **55**, No. 2, 211-218 (2019).

77. R. Turusov and V. Egorov, "Stress state and optimization of the parameters of interrupted and machine surgical sutures of human intestine," Mech. Compos. Mater., **55**, No. 3, 405-412 (2019).
78. J. Majak and S. Hannus, "Orientational design of anisotropic materials using the Hill and Tsai–Wu strength criteria," Mech. Compos. Mater., **39**, No. 6, 509-520 (2003).